View metadata, citation and similar papers at core.ac.uk

brought to you by CORE

provided by Digital Repository @ Iowa State University

IOWA STATE UNIVERSITY
Digital Repository

Agricultural and Biosystems Engineering Publications

Agricultural and Biosystems Engineering

2014

Biodegradation behavior of bacterial-based polyhydroxyalkanoate (PHA) and DDGS composites

Samy A. Madbouly
Iowa State University

James A. Schrader
Iowa State University, jschrade@iastate.edu

Gowrishankar Srinivasan
Iowa State University, srigshan@iastate.edu

Kunwei Liu
Iowa State University

Kenneth McCabe
Iowa State University, kgmccabe@iastate.edu

See next page for additional authors

Follow this and additional works at: http://lib.dr.iastate.edu/abe_eng_pubs

Part of the Bioresource and Agricultural Engineering Commons, Horticulture Commons, and the Polymer and Organic Materials Commons

The complete bibliographic information for this item can be found at http://lib.dr.iastate.edu/abe_eng_pubs/836. For information on how to cite this item, please visit http://lib.dr.iastate.edu/howtocite.html.

This Article is brought to you for free and open access by the Agricultural and Biosystems Engineering at Iowa State University Digital Repository. It has been accepted for inclusion in Agricultural and Biosystems Engineering Publications by an authorized administrator of Iowa State University Digital Repository. For more information, please contact digirep@iastate.edu.

Biodegradation behavior of bacterial-based polyhydroxyalkanoate (PHA) and DDGS composites

Abstract

The extensive use of plastics in agriculture has increased the need for development and implementation of polymer materials that can degrade in soils under natural conditions. The biodegradation behavior in soil of polyhydroxyalkanoate (PHA) composites with 10 wt% distiller's dried grains with solubles (DDGS) was characterized and compared to pure PHA over 24 weeks. Injection-molded samples were measured for degradation weight loss every 4 weeks, and the effects of degradation times on morphological, thermomechanical, and viscoelastic properties were evaluated by scanning electron microscopy (SEM), dynamic mechanical analysis (DMA), and small-amplitude oscillatory shear flow experiments. Incorporation of DDGS had a strong effect on biodegradation rate, mechanical properties, and production cost. Material weight loss increased linearly with increasing biodegradation time for both neat PHA and the PHA/DDGS 90/10 composites. Weight loss after 24 weeks was approximately six times greater for the PHA/DDGS 90/10 composites than for unaltered PHA under identical conditions. Rough surface morphology was observed in early biodegradation stages (≥8 weeks). With increasing biodegradation time, the composite surface eroded and was covered with well-defined pits that were evenly distributed, giving an areolate structure. Zero shear viscosity, Tg, gelation temperature, and cold crystallization temperature of the composites decreased linearly with increasing biodegradation time. Addition of DDGS to PHA establishes mechanical and biodegradation properties that can be utilized in sustainable plastics designed to end their lifecycle as organic matter in soil. Our results provide information that will guide development of PHA composites that fulfill application requirements then degrade harmlessly in soil.

Disciplines

Bioresource and Agricultural Engineering | Horticulture | Polymer and Organic Materials

Comments

This is a manuscript of an article published as Madbouly, Samy A., James A. Schrader, Gowrishankar Srinivasan, Kunwei Liu, Kenneth G. McCabe, David Grewell, William R. Graves, and Michael R. Kessler. "Biodegradation behavior of bacterial-based polyhydroxyalkanoate (PHA) and DDGS composites." Green Chemistry 16, no. 4 (2014): 1911-1920. DOI: 10.1039/C3GC41503A. Posted with permission.

Authors

Samy A. Madbouly, James A. Schrader, Gowrishankar Srinivasan, Kunwei Liu, Kenneth McCabe, David A. Grewell, William R. Graves, and Michael R. Kessler

This article is available at Iowa State University Digital Repository: http://lib.dr.iastate.edu/abe_eng_pubs/836

This is a post-print copy of the following article. The final version can be found at S. A. Madbouly, J. A. Schrader, G. Srinivasan, K. Liu,b K. G. McCabe, D. Grewell, W. R. Graves, M. R. Kesslera: Bidegradation Behavior of Bacterial-Based Polyhydroxyalkanoate (PHA) and DDGS Composites, *Green Chemistry*, 2014, 16(4), 1911-1920. DOI: 10.1039/C3GC41503A

Biodegradation behavior of bacterial-based polyhydroxyalkanoate (PHA) and DDGS composites

Samy A. Madbouly [ae], James A. Schrader [b], Gowrishankar Srinivasan [c], Kunwei Liu [a], Kenneth G. McCabe [b], David Grewell [c], William R. Graves [b] and Michael R. Kessler [ad]

[a]Iowa State University, Department of Materials Science and Engineering, Ames, USA. E-mail: mkessler@iastate.edu
[b]Iowa State University, Department of Horticulture, Ames, Iowa, USA
[c]Iowa State University, Department of Agricultural and Biosystems Engineering, Ames, Iowa, USA
[d]School of Mechanical and Materials Engineering, Washington State University, Pullman, WA, USA
[e]Department of Chemistry, Faculty of Science, Cairo University, Orman-Giza, Egypt

Received 27th July 2013 , Accepted 19th November 2013

Abstract: The extensive use of plastics in agriculture has increased the need for development and implementation of polymer materials that can degrade in soils under natural conditions. The biodegradation behavior in soil of polyhydroxyalkanoate (PHA) composites with 10 wt% distiller's dried grains with solubles (DDGS) was characterized and compared to pure PHA over 24 weeks. Injection-molded samples were measured for degradation weight loss every 4 weeks, and the effects of degradation times on morphological, thermomechanical, and viscoelastic properties were evaluated by scanning electron microscopy (SEM), dynamic mechanical analysis (DMA), and small-amplitude oscillatory shear flow experiments. Incorporation of DDGS had a strong effect on biodegradation rate, mechanical properties, and production cost. Material weight loss increased linearly with increasing biodegradation time for both neat PHA and the PHA/DDGS 90/10 composites. Weight loss after 24 weeks was approximately six times greater for the PHA/DDGS 90/10 composites than for unaltered PHA under identical conditions. Rough surface morphology was observed in early biodegradation stages (≥8 weeks). With increasing biodegradation time, the composite surface eroded and was covered with well-defined pits that were evenly distributed, giving an areolate structure. Zero shear viscosity, T_g, gelation temperature, and cold crystallization temperature of the composites decreased linearly with increasing biodegradation time. Addition of DDGS to PHA establishes mechanical and biodegradation properties that can be utilized in sustainable plastics designed to end their lifecycle as organic matter in soil. Our results provide information that will guide development of PHA composites that fulfill application requirements then degrade harmlessly in soil.

Introduction

Bio-based polymers and composites have received extensive attention as sustainable alternatives to petroleum-based polymers for a wide range of agricultural, industrial, and medical applications. Efforts to replace petroleum-based plastics are motivated by numerous environmental, technological, and economic problems resulting from the finite supply and increasing cost of crude oil and the environmental damage caused by heavy use of fossil carbon and disposal of non-biodegradable petroleum-based products.[1–17] Bio-based polymers have been used extensively in a wide range of industrial applications, such as textiles, resins, and rigid or flexible foams. The biodegradability and biocompatibility of these important polymers make them excellent candidates for medical applications such as drug delivery carriers and bioresorbable scaffolds for tissue engineering.[18,19] Numerous other applications for the use of bio-based polymers include food containers, waste bags, packaging, and agricultural plastics.[20,21] The use of petroleum-based plastics in agriculture is extensive, and the annual worldwide consumption of plastics for agricultural applications is estimated at more than 6.5 million tons.[22] The short service life of products such as soil-retention sheeting, agricultural films, and horticultural crop containers, and their close association with soil have generated strong interest in developing biorenewable alternatives to petroleum-based plastics that will fulfill the needed function, then biodegrade in soil under natural field conditions.[23]

Environmentally friendly bio-based polymers can be produced from a wide range of natural materials, such as carbohydrates from plants (wheat, corn, potato, sugar cane, etc.), proteins (chitin, collagen, soybean, zein, etc.), and natural oils (pine, castor, soybean, rapeseed, etc.). Many of the carbohydrate-based polymers (e.g. polylactic acid [PLA], polyhydroxyalkanoates [PHA] including polyhydroxybutyrate [PHB], polyhydroxyvalerate [PHV], and their copolymers) are synthesized via metabolic pathways of microorganisms. PHAs are the first bio-based polyesters that are highly crystalline aliphatic thermoplastics. They are produced naturally by a wide range of bacteria for carbon and energy storage.[24,25] PHAs are biodegradable polymers used in many plastics industries as replacements for petroleum-based polyethylene (PE) and polypropylene (PP) because of their excellent barrier, mechanical, and thermal properties. PHAs have also been used in blow-molded and injection-molded bottles and plastic films. In addition, PHAs are biodegradable, non-toxic and biocompatible polymers suitable for wide range of biomedical applications.[16,17] The physical and chemical properties of PHAs can be tailored for specific applications by incorporating up to 60 different types of monomers into the polymer backbone via microorganisms.[26] The hydrolysable ester bonds of PHAs enable relatively rapid degradation compared to many other bioplastics. Most PHAs are completely biodegradable and can decompose to CO_2 and H_2O through natural microbiological mineralization.[27] The depolymerization process of PHAs is facilitated by several types of microorganisms and normally yields low molecular weight products that can be absorbed as nutrients by living cells. The degradation mechanism of PHAs and their composites has been investigated in several types of media, such as soil, activated sludge, buffer solutions in laboratory atmosphere, sea water, and lake water.[28] Moisture or water content, pH, temperature, and nutrient supply are important factors that influence the degradation rate of PHAs. In addition, the chemical structure, crystallinity, surface area, and properties and amount of additives or fillers play a crucial role in the degradation kinetics of PHAs.[28]

PHAs can be blended with various biodegradable polymers and fillers, such as starch, corn stover, soy protein, and dried distillers grains with solubles (DDGS) to significantly reduce

production cost. The supply of DDGS increased dramatically in the United States from 2.7 to 32.5 million metric tons from 2000 to 2010 due to significant growth in ethanol production, which increased globally from 73.0 to 88.7 billion liters from 2009 to 2011.[29] The fibrous structure, low cost, and biodegradability of DDGS make it an attractive filler for bioplastics to enhance their mechanical properties, reduce production costs, and increase degradation rates. Incorporation of up to 30 wt% DDGS to petroleum-based polymers, such as PP and PE to produce greener composites has been studied previously.[30] In addition, DDGS have been mixed with bio-based thermoplastic polyurethane with concentrations up to 90 wt%.[31] Similarly, phenolic resin has been evaluated as a polymer binder for DDGS particles.[32,33] Polylactide has also been used as a bio-based matrix with DDGS to produce a biorenewable composite with a considerably lower production cost than pure PLA.[34]

Our objectives in the current study were to develop and evaluate commercially feasible horticultural crop containers (pots) made from a PHA/DDGS bioplastic composite with 10 wt% DDGS, to characterize the morphological, thermomechanical, and viscoelastic properties of the composite, to evaluate the effects of biodegradation on these properties, and to provide information that will guide efforts to utilize PHA/DDGS composites in products that can biodegrade and end their lifecycle as organic matter in soil. The goals for incorporating DDGS were to decrease the production cost, increase the degradation rate, and enhance the mechanical properties of PHA. The biodegradation behavior of the composite was evaluated in soil under landscape conditions for time intervals up to 24 weeks. Terrestrial-plant tests were used to evaluate toxicity of materials before and after degradation in soil. The morphologies of the composite at different biodegradation stages were studied by scanning electron microscopy (SEM), and the effect of biodegradation time on the thermomechanical properties was evaluated using dynamic mechanical analysis (DMA). In addition, the viscoelastic properties of the composite were investigated as a function of biodegradation time, temperature, and angular frequency using small-amplitude oscillatory shear flow experiments. The effect of biodegradation time on the crystallization and melting behaviors of PHA/DDGS 90/10 composite was studied using differential scanning calorimetry (DSC).

Experimental section

Materials

Compounding and injection molding. Polyhydroxyalkanoate Mirel P1003 (Injection molding grade resins) was supplied by Metabolix Inc., Cambridge, MA 02139, and the DDGS were supplied by Lincoln Way Energy LLC, Nevada, IA. This PHA contains blends of poly(R-3-hydroxybutyric acid), poly(3-hydroxybutyrate-co-4-hydroxybutyrate), proprietary mineral fillers, and proprietary biodegradable additives. DDGS is a fibrous material that contains proteins, carbohydrates, and oils and is produced as a coproduct during the dry-milling process of ethanol production. Complete drying of PHA and DDGS was accomplished for 6 h at 80 °C. Respective formulations of PHA : DDGS at 90 : 10 (w/w) were further extruded on a Leistritz compounding twin-screw extruder (Leistritz Micro18, L/D ratio 30, American Leistritz Corp., Somerville, NJ) to produce plastic extrudate that was pelletized with a pellet mill (Scheer Bay Inc. WI). The temperature profile during extrusion followed a bell profile of 125–140–130 °C from the hopper-mixing-die for all formulations. The PHA pellets were used to mold prototype 4.5-inch pots (11.5 cm OD at top and 2 mm thick) using a sprue-less mold design with an 85 ton JSW injection molding machine.

Biodegradation experiments

Biodegradation tests were carried out in soil under landscape conditions at the Horticulture Research Station near Gilbert, IA. Samples of PHA and PHA/DDGS 90/10 composite were one-fourth container pieces (injection molded plant containers with a top diameter of 11.4 cm, height of 9.7 cm, and volume of 680 cm^3, cut into four identical pieces). Each sample was weighed, placed in a non-degradable mesh bag for easy retrieval, and buried 10 cm below the soil surface in a garden plot in a randomized complete block design. Each block represented a group of samples to be randomly selected for extraction from soil at a designated time interval (every 4 weeks for up to 24 weeks). The soil type was Clarion loam, a fine-loamy, mixed, superactive, mesic Typic Hapludolls. During the trial, the mean 10 cm soil temperature was 21.1 °C, and the landscape plot was irrigated uniformly once per week with ≈2.5 cm of water. After each biodegradation time interval, samples were extracted from the soil, washed with water under gentle agitation, dried at 33 ± 5 °C and mean RH of 26% for 9 d, then held for 24 h in the same room where the initial weight was measured to reach equilibrium with ambient humidity. Percentage weight loss after each degradation time interval was calculated from the following equation:

$$W_{loss}\% = \frac{W_0 - W_1}{W_0} \times 100$$

where W_{loss}% is the relative weight loss, W_0 is the weight of the sample before biodegradation step. W_1 is the weight of the biodegraded sample after washing with water and drying until reaching a constant weight.

Samples were tested for phytotoxicity before and after degradation in soil by using the OECD terrestrial plant test of seedling emergence and seedling growth.[35] Germination and seedling-growth tests were performed with tomato (Solanum lycopersicum L.) by grinding the PHA and PHA/DDGS 90/10 composite test materials into particles ≤1 mm diameter, mixing the ground material with soil at 1000 or 10 000 ppm by weight, and culturing seeds and seedlings in the media mixtures for a total of 27 days in a greenhouse in a completely randomized experimental design with control units grown in the same soil without addition of test materials. Experimental units were evaluated for presence or absence of phytotoxic effects by measuring percentage of seedling emergence and seedling height, and by visual inspection of seedlings for evidence of stunted growth, chlorosis, discoloration, mortality, or abnormal morphology.[35]

Scanning electron microscopy

The surface morphology of PHA/DDGS composites was examined using SEM after six different durations of biodegradation in soil (0, 8, 12, 16, 20, and 24 weeks). The samples were fixed on the SEM holders and sputtered with gold. The prepared samples were investigated using a field-emission scanning electron microscope (FE-SEM, FEI Quanta 250) operating at 10 kV under high vacuum.

Rheological measurements

The effect of biodegradation on the dynamic viscosity and crystallization behavior was investigated using a TA Instruments, AR2000ex rheometer, with 25 mm diameter parallel plates. All measurements were performed under very accurate thermal conditions (±0.1 K) using an air/N_2 gas convection oven designed with twin element heater guns, a barrel-shaped chamber, and three internal platinum resistance

thermometers (PRT) for optimum temperature stability. The following rheological experiments were studied:

1. Strain sweep at 160 °C and constant angular frequency to obtain the linear viscoelastic regime of the composites.

2. Angular frequency sweep at 160 °C to evaluate the complex viscosity after different biodegradation time intervals.

3. A temperature sweep (2 °C min^{-1} cooling rate) at a constant angular frequency and a certain strain rate in the linear viscoelastic regime to evaluate the crystallization or gelation temperature at different biodegradation time intervals.

DMA measurements

The DMA measurements after different biodegradation times were carried out using a Q800 dynamic mechanical analyzer. Rectangular shape samples of 0.77 mm thick and 8 mm wide were heated from −90 to 100 at 2 °C min^{-1} heating rate at a frequency of 1 Hz.

DSC measurements

Standard DSC measurements were carried out using a TA Instruments Q2000 to investigate the effect of biodegradation on the melting and crystallization behavior of PHA/DDGS composites. All DSC measurements were performed in an atmosphere of dry nitrogen. The melting temperature (T_m) of all samples at different biodegradation stages was evaluated using the maximum of the endothermic melting peak at a heating rate of 10 °C min^{-1}. To study the effect of biodegradation on the crystallization temperature (T_c), the samples were rapidly heated above their T_m and annealed for 3 min to erase the thermal history. The molten samples were cooled at 10 °C min^{-1}, and the T_c was determined from the maximum of the exothermic crystallization peak.

Results and discussion

With the current average industry price of PHA at approximately $2.50 per lb and the price of DDGS at approximately $0.11 per lb,[36,37] substituting a percentage of PHA with DDGS to form a composite can offer substantial savings. For our prototype plant containers, replacement of 10 wt% of PHA with DDGS brought a savings of 9.6% for material cost, and our trials suggest that the percentage of DDGS could be increased to 20% or more without reducing the performance of the prototypes for this application.

Biodegradation time dependence of weight loss for unaltered PHA and PHA/DDGS 90/10 composites in soil medium is shown in Fig. 1. These results indicate that the biodegradation of PHA can be significantly accelerated by adding a small amount of DDGS. Weight loss after 24 weeks of biodegradation time in soil is about six times greater for the PHA/DDGS 90/10 composite than for unaltered PHA under identical biodegradation conditions. Therefore, addition of DDGS not only decreases the cost of PHA-based material required for an agricultural-plastics application, it also enhances the degradation process when it is included at a rate as low as 10% of the composite (Fig. 1). DDGS contain high amounts of protein, fiber, amino acids, and other nutrients that can be easily biodegraded in soil. The favorable interaction between PHA and DDGS is also an important factor for the high biodegradation rate of the composite compared to unaltered PHA.

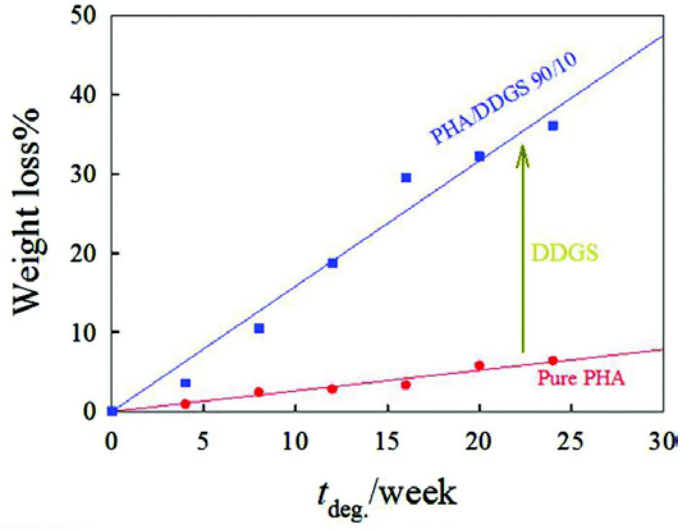

Fig. 1 Biodegradation time dependence of weight loss of unaltered PHA and PHA/DDGS 90/10 composites in soil medium.

Optical images for one-fourth plant containers of unaltered PHA before biodegradation and unaltered PHA and PHA/DDGS 90/10 composite after 24 weeks in soil are shown in Fig. 2. Degradative damage and weight loss were minimal for unaltered PHA, but significant damage and greater weight loss were observed for the PHA/DDGS 90/10 composite after 24 weeks biodegradation time. These results compare well with the biodegradation behavior of PCL/clay nanocomposite reported by Singh et al.,[38] where the biodegradation rate of PCL was enhanced significantly by adding a small amount of clay as nanofiller. After 60 days biodegradation time, the PCL/clay composite became brittle and difficult to recover from the compost. The higher biodegradation rate in the presence of nanoclay was attributed to the presence of hydroxyl groups on the edges of montmorillonite, which can catalyze faster hydrolytic degradation of the PCL matrix.[38] This comparatively higher biodegradation rate of PCL/nanoclay composite was also presumably due to the high interaction between PCL and nanoclay, as evident from decreasing the heat of fusion and crystallinity similar to our current system (PHA/DDGS composite).[38] Biodegradation of PHA/DDGS is likely also enhanced by the favorable change in nutrient components for microbes compared to the PHA alone. The proteins and amino acids from the DDGS provide nitrogen (N) and improve the carbon-to-nitrogen (C : N) ratio of the material. While the nitrogen content of PHA is negligible, making it difficult for microbes to begin degradation, the N content of DDGS is approximately 4.1% and it has a C : N ratio of 12 : 1.[39] Therefore, our PHA/DDGS 90/10 composite material has a C : N ratio of approximately 114 : 1, a ratio that is much more conducive to biodegradation considering the optimum ratio for the start of industrial composting is 30 : 1.[40]

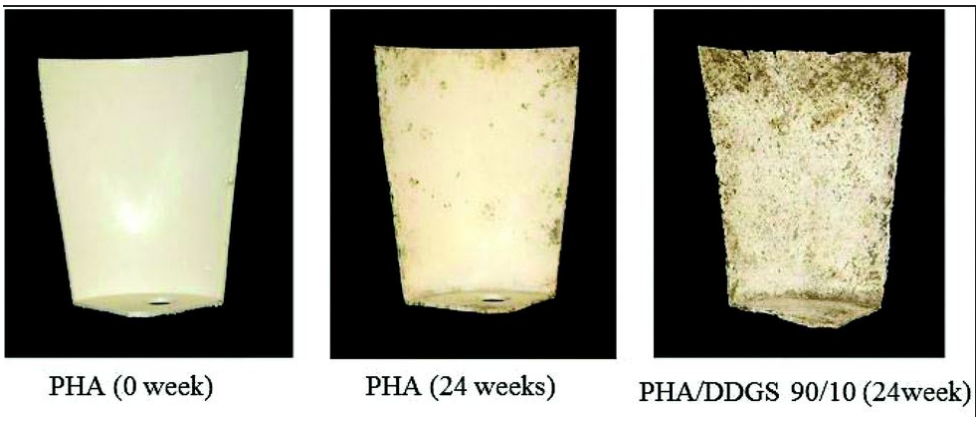

Fig. 2 Photographs of unaltered PHA and PHA/DDGS 90/10 composite samples (one-fourth plant containers) before and after 24 weeks of degradation time in soil medium

Our tests for phytotoxicity showed no adverse effects of PHA or the PHA/DDGS 90/10 composite material on seed germination or seedling growth for either new, non-degraded, materials or materials degraded in soil for 24 weeks. The test plant (tomato) grown in medium containing PHA and PHA/DDGS 90/10 at 1000 or 10 000 ppm showed 100% germination, no reduction in seedling height compared to controls, and no visual evidence of phytotoxicity. Fig. 3 shows a typical comparison for test plants grown in a bioplastic container (pot) made from PHA/DDGS 90/10 composite and a commercially-available (control) container made of petroleum-based PP. Healthy plants with nearly identical growth rate were observed consistently in both container types. These results indicate that the biodegradable PHA/DDGS 90/10 composite can be used as a high-quality alternative for petroleum-based polymers in horticultural crop containers.

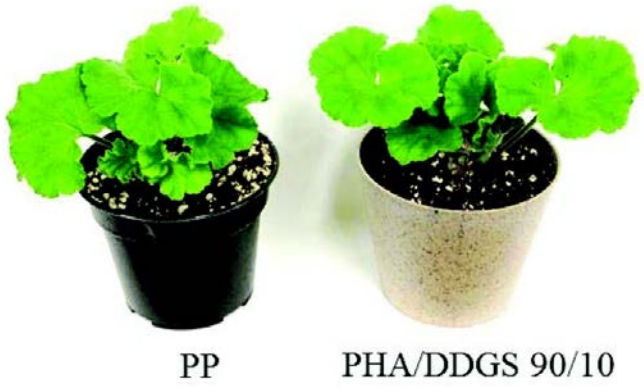

Fig. 3 Photograph of test plants (geranium) growing in a control (PP) container and a PHA/DDGS 90/10 composite container. Test plants showed consistent health and nearly identical growth rate in the two container types.

Optical microscope (OM), scanning electron microscopy (SEM) and atomic force microscopy (AFM) are well established techniques widely used to evaluate the effect of biodegradation on the internal structure or morphology of biodegradable polymers.[41–45] In addition, Fourier

transform infrared spectroscopy (FT-IR), X-ray, and dielectric sorption analysis (DSA)[46–49] have been successfully employed to study the chemical changes to the polymer surface due to scission of chemical bonds after the biodegradation process. For the PHA/DDGS composite, the surface morphology was investigated at different stages of biodegradation. Fig. 4 shows typical surface morphologies for samples that were biodegraded in soil medium for different biodegradation times, t_d = 0, 8, 12, 16, 20, and 24 weeks. A very smooth surface morphology was observed for the composite before starting the biodegradation process (t_d = 0 week). In the early stage of the biodegradation process (t_d = 8 weeks) numerous cracks in the surface of the composite were observed. With increasing biodegradation time, the cracks became deeper and the surface eroded and became covered with well-defined pits, which were evenly distributed, giving an areolate appearance. Fig. 5 shows the SEM micrographics for the PHA/DDGS 90/10 composite after t_d = 24 weeks at different magnifications. It is apparent that the erosion pits became deeper and aggregated to form large eroded regions with many irregular small pieces, and consequently led to a significant weight loss as presented in Fig. 1.

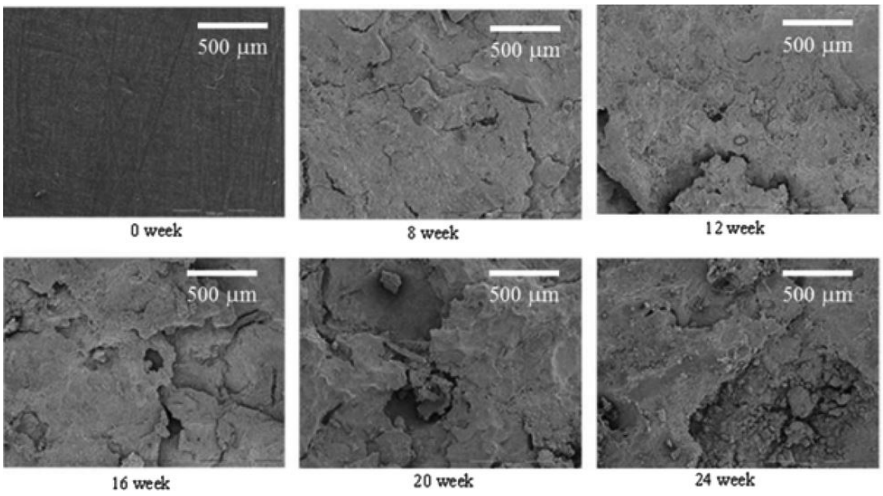

Fig. 4 SEM micrographs of surface morphologies of PHA/DDGS 90/10 composites after different durations of biodegradation in soil.

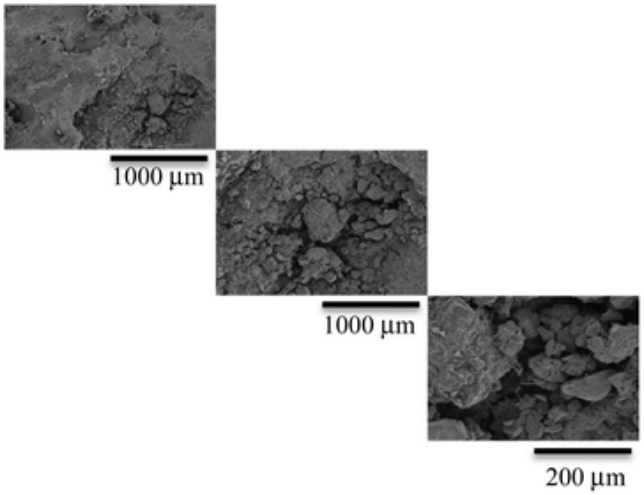

Fig. 5 SEM micrographs of surface morphology of PHA/DDGS 90/10 composite after 24 weeks biodegradation time at different magnifications

The DMA measurements for the PHA/DDGS composites after different biodegradation time intervals were investigated to evaluate the effect of different biodegradation stages on the thermomechanical properties of the composite. Fig. 6 shows the dynamic storage and loss moduli, E′ and E″, respectively, as a function of temperature for different biodegradation time intervals up to 20 weeks. The sample after 24 weeks is not included in the DMA measurements because it is too brittle to prepare reliable dimensions for the DMA test. Two relaxation processes have been observed for this composite in this temperature range. The first process that appears around 17 °C for the non-degraded sample (0 weeks) is related to the glass relaxation processes (α-relaxation) of the composite. The peak maximum (T_{max}) of the α-relaxation process (see the E″ versus T) shifted systematically to lower temperature with increasing biodegradation time. The inset-plot shows a linear behavior of T_{max}versus biodegradation time. This experimental fact suggests that the T_g of the composite decreased linearly with increasing biodegradation time in soil medium under typical landscape conditions. The second relaxation process appears at approximately 125 °C, which is normally associated with most crystalline and semi-crystalline polymers and related to the slippage of the crystallites past each other. This process is not significantly affected by different biodegradation times as clearly seen in Fig. 6. It is also apparent that the value of E′ decreases systematically with increasing biodegradation time over a wide range of temperatures, an outcome that is typically related to the decrease in the molecular weight of the sample as a result of biodegradation. The value of E′ decreases linearly with increasing biodegradation time at −190 °C, as clearly seen in the inset-plot of Fig. 6. At higher temperatures ($T \geq 165$ °C), both E′ and E″ decrease very sharply due to the melting of the crystalline region in the composite. At this high temperature, large-scale chain slippage occurs and the material flows.

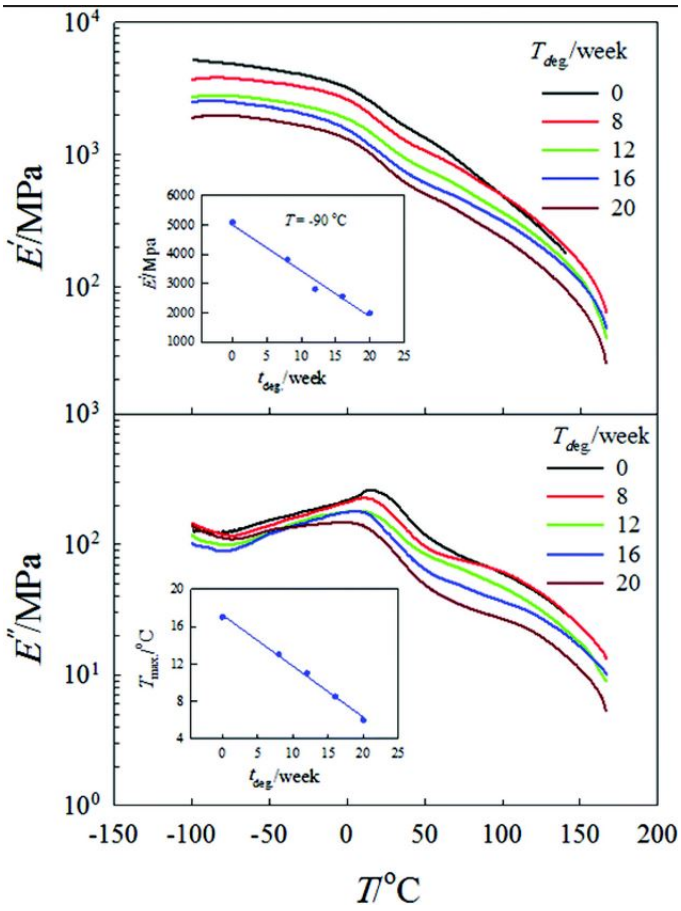

Fig. 6 Dynamic storage, E′, and loss, E″, moduli as a function of temperature at a frequency of 1 Hz and 2 °C min^{-1} heating rate for PHA/DDGS 90/10 composite after different durations of biodegradation in soil medium under typical landscape conditions. The inset-plots show the biodegradation time dependence of E′ at −90 °C and the T_{max} of the α-relaxation process as a function of biodegradation time.

The biodegradation process of the PHA/DDGS 90/10 composite may have a significant influence on the viscoelastic properties. For this reason, the rheological behavior of this composite was studied as a function of biodegradation time, temperature, and angular frequency using small-amplitude oscillatory shear flow experiments. Fig. 7 shows the classical angular frequency dependence of complex viscosity, η*, at 170 °C for PHA/DDGS 90/10 composite after different durations of biodegradation. Clearly, η* decreased systematically with increasing biodegradation time. The η* decreased by almost one order of magnitude after 24 weeks biodegradation time as seen in Fig. 7. It is also clear that η* became less angular-frequency dependent (more Newtonian behavior) with increasing biodegradation time.

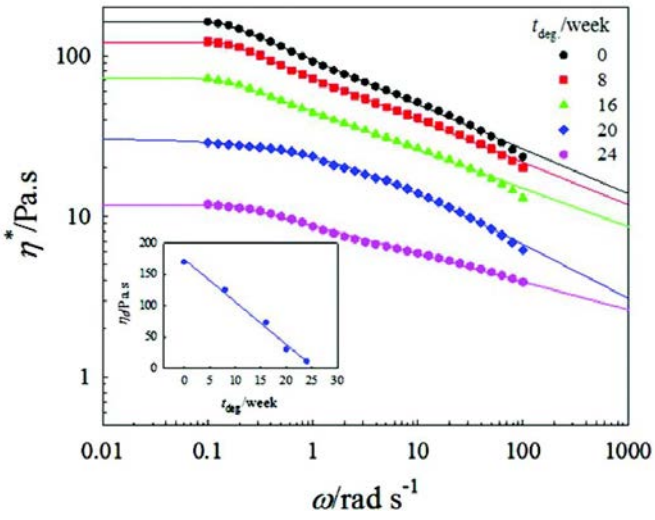

Fig. 7 Angular frequency dependence of complex viscosity at 170 °C for PHA/DDGS 90/10 composites after different durations of biodegradation in soil under typical landscape conditions. The solid lines are calculated from eqn (2) by using nonlinear regression analysis. The inset-plot shows the biodegradation time dependence of zero shear viscosity.

The η* dependence of angular frequency can be expressed by several models, such as the Carreau–Yasuda model, according to the following equation:[50]

$$|\eta^*| = \eta_0[1 + (\tau_\eta \omega)^a]^{(n-1)/a}$$

where τ_η is a characteristic viscous relaxation time that defines the location of the transition from Newtonian to shear-thinning behavior, while n and a are material constants. The zero-shear viscosity, η_0, can be calculated as a fitting parameter to the experimental results using nonlinear regression analysis. An excellent description of the data was obtained as shown in Fig. 7 by using the above equation, where the lines are fitting lines and the symbols are the experimental data. The inset-plot of Fig. 7 shows the biodegradation time dependence of η_0 obtained from the above analysis. Clearly η_0 decreased linearly with increasing biodegradation time similar to the decrease of E′ and peak maximum (T_{max}) of the α-relaxation process as already mentioned above.

Dynamic rheology has been successfully used to investigate the crystallization behavior and kinetics of semicrystalline polymers.[51–56] The onset of crystallization of PP, PE, and PP/PE blends have been detected rheologically by Teh et al.[51] In addition, semiqualitative information about the nucleation density and initial crystallization rate have also been deduced from rheological data. Furthermore, the obtained results were consistent with differential scanning calorimetry (DSC) and optical microscopy data. The rheological mechanism and an overview of nucleated crystallization kinetics of PP in the presence of a nucleating agent have been studied by Khanna,[52] who found that the rheological technique for studying crystallization kinetics was more sensitive than conventional techniques like DSC. Other research has evaluated the isothermal crystallization behavior of biodegradable poly(ε-caprolactone), PCL, as functions of crystallization temperature, shear rate, and shearing time.[57] It was found that the crystallization

process was accelerated to a great extent under high shear rate and long shearing time. The induction time of the crystallization process was found to substantially decreased with increasing shear rate. The isothermal crystallization kinetics at various shear rates was also analyzed using the Avrami equation.[57]

The effect of soil biodegradation on the crystallization behavior of PHA/DDGS 90/10 composite can be investigated from the dynamical cooling sweep at a constant cooling rate and angular frequency. Fig. 8 demonstrates the simultaneous temperature dependence of the dynamic shear moduli, G′ and G″ at 2 °C min^{-1} cooling rate and 10 rad s^{-1} angular frequency for the non-degraded PHA/DDGS 90/10 composite. It is apparent that both G′ and G″ are very sensitive to the structure change accompanying the crystallization process. At T ≥ 150 °C, both G′ and G″ are almost temperature independent and G″ is approximately one order of magnitude higher than G′, indicating that the composite has a liquid-like behavior at this temperature range. The values of G′ and G″ slightly increase with decreasing temperature at 140 °C ≥ T ≥ 150 °C. At temperatures lower than 140 °C, sudden increase in the values of both G′ and G″ by several orders of magnitude was observed. This dramatic increase in G′ and G″ at this low temperature range (T < 140 °C) was related to the onset of crystallization and the formation of the physical gel of the crystalline structure of PHA. At much lower temperature (T ≤ 134 °C), both G′ and G″ reached constant values and G′ became more than one order of magnitude higher than G″ due to the formation of equilibrium moduli of the crystalline structure of the composite. The value of gelation temperature, T_{gel} due to the formation of solid-like structure resulting from the crystallization process of PHA can be accurately identified from the crossover point of G′ and G″, as indicated by the arrow in Fig. 8.

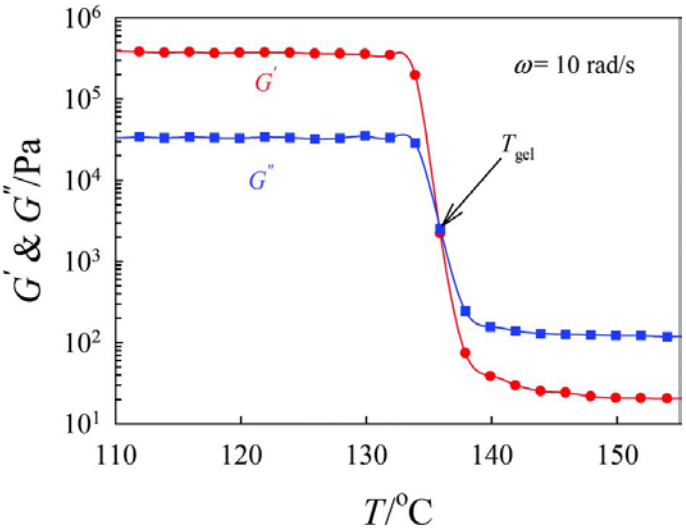

Fig. 8 Temperature ramps of G′ and G″ for the non-degraded PHA/DDGS 90/10 composite at 2 °C min^{-1} cooling rate and 10 rad s^{-1} angular frequency. The arrow indicates the gelation temperature, T_{gel}.

Fig. 9 shows the temperature dependence of η* and loss tangent (tan δ). Clearly, the complex viscosity increased dramatically once the crystallization process started to take place, a result similar to the variation of G′ and G″ with temperature (see Fig. 8). However, tan δ decreased by about two orders of magnitude, which reflects a greater sensitivity of G′ than G″ to the crystallization process (tan δ = G″/G′).

This substantial change in the rheological parameters during the crystallization process can be attributed to the continuous increase of the volume fraction of the crystalline part that may act like cross-links, hence increasing the G′, G″, and η* as well as decreasing tan δ of the sample from the melt to the solid crystalline state.

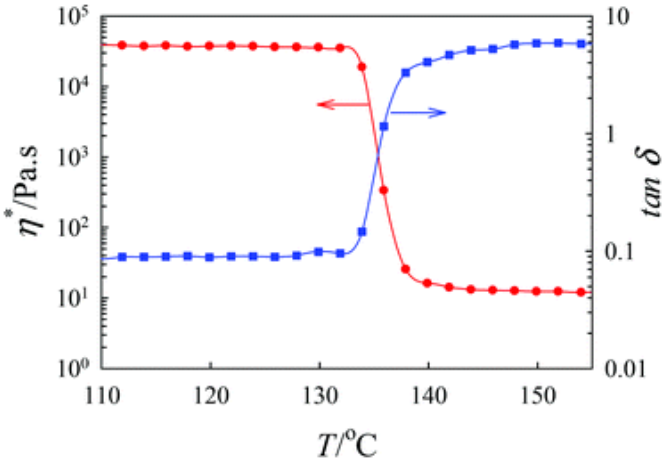

Fig. 9 Temperature ramps of η* and tan δ, for the non-degraded PHA/DDGS 90/10 composite at 2 °C min^{-1} cooling rate and 10 rad s^{-1} angular frequency.

Fig. 10 and 11 show the temperature dependence of G′ and η* for the PHA/DDGS 90/10 composite at 2 °C min^{-1} cooling rate and 10 rad s^{-1} angular frequency as a function of biodegradation time. The results show that biodegradation time can significantly affect the crystallization process of the PHA composite, and reveal that the longer the biodegradation time, the lower the temperature at which both η* and G′ increase strongly. For example, the onset temperature at which both η* and G′ increase for the non-degraded sample ($t_{deg.}$ = 0 week) was about 8 °C higher than the corresponding value for the sample that was biodegraded for 20 weeks. This experimental fact suggests that the biodegradation process in soil medium decreases the crystallization kinetics and/or the crystallization percentage of PHA. The T_{gel} obtained from the crossover point of G′ and G″ (as described in Fig. 8) was found to be strongly influenced by biodegradation time. Fig. 12 demonstrates the biodegradation time dependence of T_{gel}, showing that T_{gel} decreased linearly with increasing biodegradation time.

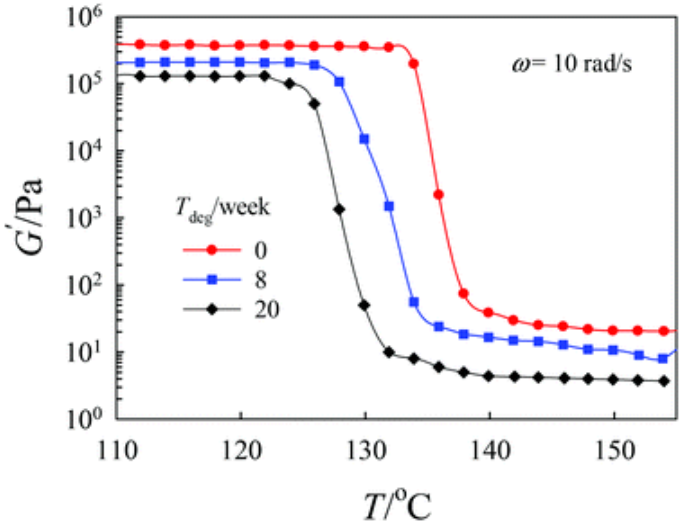

Fig. 10 Temperature ramps of G′ for PHA/DDGS 90/10 composites that were biodegraded in soil medium for different time intervals. The measurements were carried out at 2 °C min^{-1} cooling rate and 10 rad s^{-1} angular frequency.

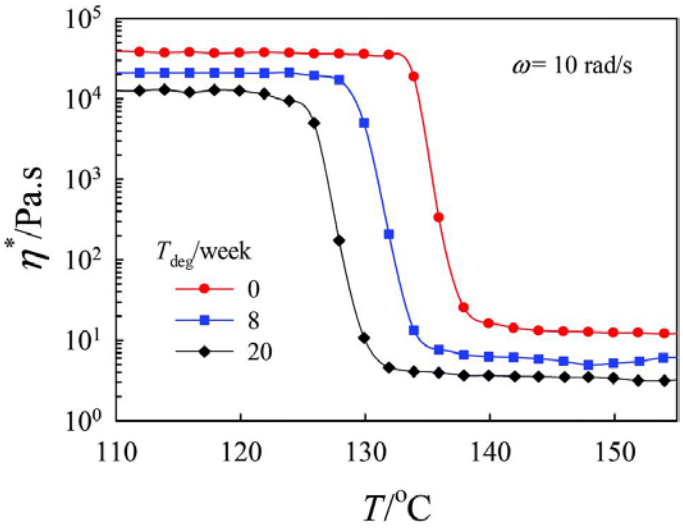

Fig. 11 Temperature ramps of η* for PHA/DDGS 90/10 composites that were biodegraded in soil medium for different time intervals. The measurements were carried out at 2 °C min^{-1} cooling rate and 10 rad s^{-1} angular frequency.

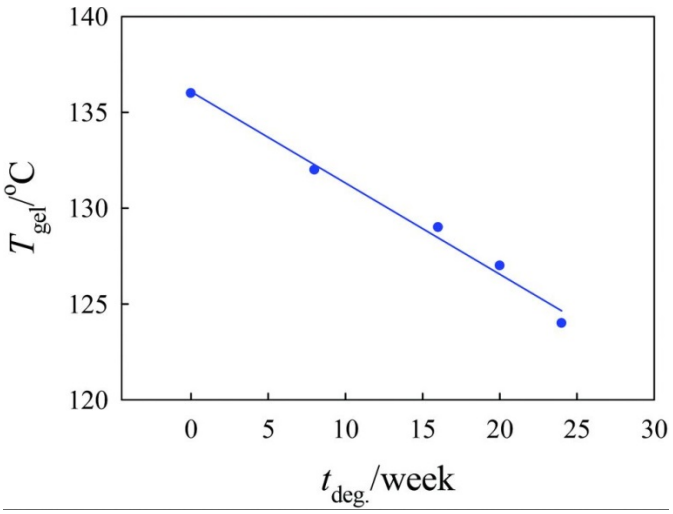

Fig. 12 Biodegradation time dependence of T_{gel} for the PHA/DDGS 90/10 composite. The T_{gel} was determined from the cross over point of G′ and G″ at 2 °C min^{-1} cooling rate and 10 rad s^{-1} angular frequency.

It is expected that structural parameters such as lamellar thickness, crystal interphase, and spherulitic growth rates are substantially modified by decreasing the molecular weight during the biodegradation process due to the changes in the free energy required for the formation of crystals. The DSC thermographs (first heating run) of the PHA/DDGS 90/10 composite as a function of biodegradation time are shown in Fig. 13. The curves displayed two endothermic peaks due to primary and secondary crystallization processes for all composites regardless of the level of biodegradation. These bimodal melting peaks also confirmed the existence of melt-recrystallization mechanisms. During heating of the sample in the DSC, the less perfect crystals melted at lower temperatures and then the samples reorganized into more perfect crystals that melt at higher temperatures. The biodegradation has a significant effect on the melting enthalpy (ΔH_m) and the degree of crystallinity (DOC) of the composite. The ΔH_m calculated from the area under the two bimodal melting peaks was presented as a function of biodegradation time. ΔH_m decreased exponentially with increasing biodegradation time as seen in the inset-plot of Fig. 13.

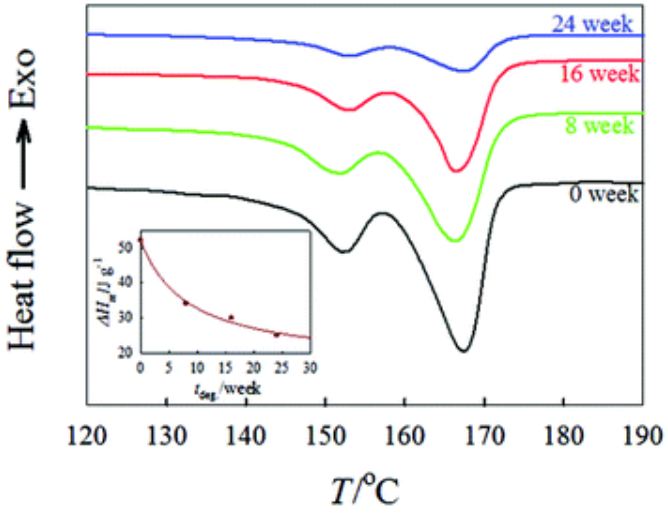

Fig. 13 Development of melting temperature of the PHA/DDGS composites at different durations of biodegradation in soil. The DSC measurements were carried out at 10 °C min^{-1} heating rate (first heating run). The inset-plot shows the biodegradation time dependence of heat of fusion calculated from the data presented in Fig. 13.

These results suggest that the biodegradation of the PHA/DDGS composites has a substantial effect on the degree of crystallinity. Specifically, the degree of crystallinity decreases with increasing biodegradation time. Based on these results it is apparent that the biodegradation process of the PHA/DDGS 90/10 composite in soil medium takes place in both crystalline and amorphous regions, resulting in an overall decrease in the crystallization behavior. A considerable decrease in the degree of crystallinity as a result of hydrolytic degradation of poly-L-lactide (PLLA) has been reported for samples that were crystallized at 90 °C by Iannace et al.[58] For PLLA, the biodegradation process advanced in both the crystalline and amorphous regions, resulting in an overall decrease of the degree of crystallinity similar to that seen for the PHA/DDGS 90/10 composite in our work.

The significant heat release accompanying the exothermic cold crystallization process of PHA/DDGS can be easily evaluated using DSC. The heat released is directly related to the macroscopic rate of the crystallization process. A typical cold crystallization process for the PHA/DDGS 90/10 composite as a function of biodegradation time is shown in Fig. 14. The sample was melted at T = 200 °C for 3 min to erase the thermal history and then cooled to 0 °C at a 10 °C min^{-1} cooling rate. A sharp cold-crystallization process was observed for the non-degraded sample (t_d = 0 week) with crystallization peak maximum at approximately T_c = 111 °C. The value of T_c decreased linearly with increasing biodegradation time, as seen in the inset-plot of Fig. 14. In addition, bimodal crystallization peaks were detected for the samples at longer biodegradation times ($t_d \geq 16$ weeks). The crystallization peaks observed at low temperature (T_c = 90 °C) for the two samples that were biodegraded for 16 and 24 weeks might be related to the formation of low molecular weight fragments that can crystallize at lower temperature compared to high molecular weight fragments. This low temperature crystallization peak was not observed for composites at t_d = 0 and 8 weeks due to the presence of well-developed crystals. These DSC data are in good agreement with the rheological behavior described above. Based on the preceding discussion it is apparent that both DSC and rheology studies confirmed that biodegradation of the PHA/DDGS 90/10 composite can significantly inhibit the crystallization behavior (i.e., slowing the crystallization kinetics and decreasing the crystallization percentage).

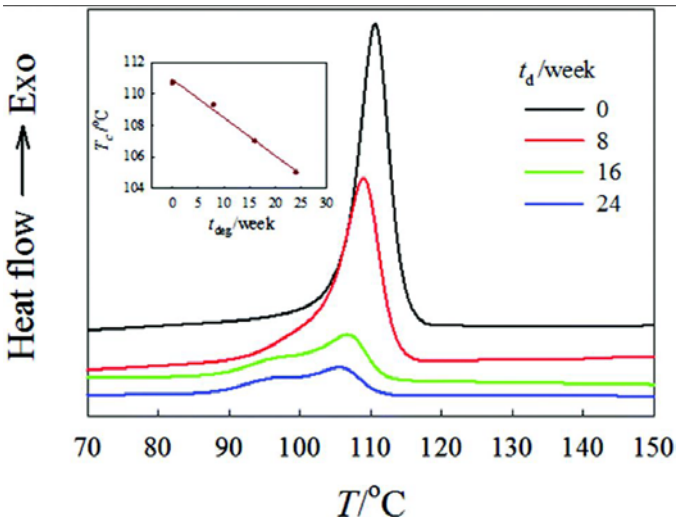

Fig. 14 Development of cold crystallization processes for the PHA/DDGS 90/10 composite at different durations of biodegradation in soil. The DSC measurements were carried out at 10 °C min^{-1} cooling rate. The inset-plot shows the degradation time dependence of crystallization temperature calculated from the data presented in Fig. 10 and 11.

Conclusions

Addition of DDGS to PHA to form a composite establishes mechanical and biodegradation properties that can be utilized in sustainable plastics designed to end their lifecycle as organic matter in soil, characteristics that could be especially useful for agricultural-plastics applications. Adding DDGS can decrease material costs, increase the biodegradation rate, and enhance the mechanical properties of PHA. Both PHA and the PHA/DDGS 90/10 composite were found to be non-toxic to plants before and after 24 weeks of biodegradation in soil, confirming the suitability of the materials for agricultural applications. The biodegradation process was found to have a significant influence on the thermomechanical and viscoelastic properties of PHA/DDGS 90/10 composite. The zero shear viscosity, elastic modulus, and peak maximum of the glass relaxation process decreased linearly with increasing biodegradation time due to the decrease in the molecular weight of the sample as a result of biodegradation. The DSC and rheological investigations revealed that biodegradation of the PHA/DDGS 90/10 composite in soil medium took place in both crystalline and amorphous regions, and consequently the degradation slows the crystallization kinetics and decreases the crystallization percentage.

Acknowledgements

This research was supported in part by the USDA Specialty Crops Research Initiative (USDA-SCRI project # IOW05306). We thank Metabolix, Inc. for providing Mirel PHA, and we thank R&D/Leverage Company for their valuable assistance and technical support during injection molding of prototype containers. We also thank Kyle Haubrich and Samuel Schrader for their technical assistance during prototype development, trial establishment, and data collection.

References

1. J. A. Stagner, S. Tseng and E. K. L. Tam, J. Polym. Environ., 2012, 20, 1046–1051
2. F. X. Xia, X. L. Wang, F. Song and Y. Z. Wang, J. Polym. Environ., 2012, 20, 1103–1111
3. C. Kongkaew, C. Dokkhan, S. Pattanawanidchai, O. Chaikumpollert and S. Loykulnant, Biomass Bioenergy, 2012, 46, 233–241
4. G. Stoclet, M. Sclavons and J. Devaux, J. Appl. Polym. Sci., 2013, 127, 4809–4824
5. J. D. Badia, L. Santonja-Blasco, A. Martinez-Felipe and A. Ribes-Greus, Bioresour. Technol., 2012, 111, 468–475
6. A. Mudhoo, R. Mohee, G. D. Unmar and S. K. Sharma, RSC Green Chemistry Series (Handbook of Applied Biopolymer Technology), 2011, vol. 12, pp. 332–364
7. T. A. Osswald and S. Garcia-Rodriguez, RSC Green Chemistry Series (Handbook of Applied Biopolymer Technology), 2011, vol. 12, pp. 1–21
8. E. Chiellini, A. Corti, S. D'Antone and D. M. Wiles, in Handbook of Biodegradable Polymers, ed. A. Lendlein and A. Sisson, Wiley, Hoboken, NJ, 2011, pp. 379–398
9. S. J. Park, S. Y. Lee, T. W. Kim, Y. K. Jung and T. H. Yang, Biotechnol. J., 2012, 7, 199–212
10. S. Modi, K. Koelling and Y. Vodovotz, J. Appl. Polym. Sci., 2012, 124, 3074–3081
11. F. Song, D. L. Tang, X. L. Wang and Y. Z. Wang, Biomacromolecules, 2011, 12, 3369–3380
12. E. Rudnik and D. Briassoulis, Ind. Crops Prod., 2011, 33, 648–658
13. A. Campanella, J. J. La Scala and R. P. Wool, J. Appl. Polym. Sci., 2011, 119, 1000–1010
14. M. I. Aranguren, N. E. Marcovich and M. A. Mosiewicki, in Green Composites, ed. F. Willems and P. Moens, 2010, pp. 99–118
15. H. Ariffin, H. Nishida, M. A. Hassan and Y. Shirai, Biotechnol. J., 2010, 5, 484–492
16. D. B. Hazer, E. Kilicay and B. Hazer, Mater. Sci. Eng., C, 2012, 32, 637–647
17. B. Hazer and A. Steinbüchel, Appl. Microbiol. Biotechnol., 2007, 74, 1–12
18. M. Mucha and M. Tylman, Adv. Mater. Res., 2012, 488–489, 681–685 .
19. H. Y. Cheung, K. T. Lau, T. P. Lu and D. Hui, Composites, Part B, 2007, 38, 291–300
20. S. Kalia, B. S. Kaith and S. Vashistha, in Handbook of Bioplastics and Biocomposites Engineering Applications, ed. S. Pilla, Wiley-Scrivener, 2011, pp. 453–470
21. D. Rusu, S. A. E. Boyer, M. F. Lacrampe and P. Krawczak, in Handbook of Bioplastics and Biocomposites Engineering Applications, ed. S. Pilla, Wiley-Scrivener, 2011, pp. 397–449
22. G. Scarascia-Mugnozza, C. Sica and G. Russo, J. Ag. Eng. - Riv. Ing. Agr., 2011, 3, 15–28
23. D. Grewell, G. Srinivasan, J. Schrader, W. Graves and M. Kessler, SPE-ANTEC Tech. Pap., 2013, 59
24. R. A. J. Verlinden, D. J. Hill, M. A. Kenward, C. D. Williams and I. Radecka, J. Appl. Microbiol., 2007, 102, 1437–1449
25. G. Braunegg, G. Lefebvre and K. F. Genser, J. Biotechnol., 1998, 65, 127–161
26. K. Sudesh, H. Abe and Y. Doi, Prog. Polym. Sci., 2000, 25, 1503–1555
27. J. Y. Chee, S. S. Yoga, N. S. Lau, S. C. Ling, R. R. M. Abed and K. Sudesh in Current Research, Technology and Education Topics in Applied Microbiology and Microbial Biotechnology, ed. A. Méndez-Vilas, Formatex Research Center, Spain, 2010, pp. 1395–1404
28. A. P. Bonartsev V. L. Myshkina, D. A. Nikolaeva, E. K. Furina1, T. A. Makhina, V. A. Livshits, A. P. Boskhomdzhiev, E. A. Ivanov, A. L. Iordanskii and G. A. Bonartseva, in Current Research, Technology and Education Topics in Applied Microbiology and Microbial Biotechnology, ed. A. Méndez-Vilas, Formatex Research Center, Spain, 2007, pp. 295–237
29. A. K. Mohanty, N. Zarrinbakhsh and M. Misra, 18th International Conference On Composite Materials, Korea, 2011 .
30. J. L. Julson, G. Subbarao, D. D. Stokke, H. H. Gieselman and K. Muthukumarappan, J. Appl. Polym. Sci., 2004, 93, 2484–2493
31. Q. Wu and A. K. Mohanty, J. Biobased Mater. Bioenergy, 2007, 1, 257–265

32. R. A. Tatara, E. S. Suraparaju and K. A. Rosentrater, J. Polym. Environ., 2007, 15, 89–95
33. V. Cheesbrough, K. Rosentrater and J. Visser, J. Biobased Mater. Bioenergy, 2008, 16, 40–50
34. Y. Li and X. S. Sun, J. Appl. Polym. Sci., 2001, 121, 589–597
35. OECD, OECD Guidelines for the Testing of Chemicals, OECD Publishing, 2006, DOI:10.1787/9789264070066-en .
36. D. de Guzman, Green Chem. Blog., Nov. 11, 2012.
37. USDA-MO Dept. Ag. Market News. May 28, 2013.
38. N. K. Singh, B. D. Purkayastha, J. K. Roy, R. M. Banik, M. Yashpal, G. Singh, S. Malik and P. Maiti, ACS Appl. Mater. Interfaces, 2010, 2, 69–81
39. A. D. Moore, A. K. Alva, H. P. Collins and R. A. Boydston, Commun. Soil Sci. Plant Anal., 2010, 41, 1315–1326
40. T. Richard and N. Trautmann, Cornell Composting Science and Engineering, http://compost.css.cornell.edu/science.html, May 30, 2013.
41. E. Franco-Marques, J. A. Mendez, J. Girones and M. A. Pelach, J. Appl. Polym. Sci., 2013, 128, 3455–3464
42. D. S. Dias, M. S. Crespi, M. Kobelnik and C. A. Ribeiro, J. Therm. Anal. Calorim., 2009, 97, 581–584
43. J. M. Cangemi, N. S. Claro, G. O. Chierice and A. M. dos Santos, Polim.: Cienc. Tecnol., 2006, 16, 129–135
44. M. Fujita, Y. Kobori, Y. Aoki, N. Matsumoto, H. Abe, Y. Doi and T. Hiraishi, Langmuir, 2005, 21, 11829–11835
45. A. G. Shard, K. M. Shakesheff, C. J. Roberts, S. B. Tendler and M. C. Davies, in Handbook of Biodegradable Polymers, ed. A. J. Domb, J. Kost and D. Wiseman, CRC Press, 1998, pp. 417–450
46. J. Sahari, S. M. Sapuan, E. S. Zainudin and M. A. Maleque, Carbohydr. Polym., 2013, 92, 1711–1716
47. E. Abraham, P. A. Elbi, B. Deepa, P. Jyotishkumar, L. A. Pothen, S. S. Narine and S. Thomas, Polym. Degrad. Stab., 2012, 97, 2378–2387
48. M. Giacomelli Penon, S. J. Picken, M. Wubbenhorst and J. van Turnhout, Polym. Degrad. Stab., 2007, 92, 1857–1866
49. M. Penon, Giacomelli, S. J. Picken, M. Wuebbenhorst and J. van Turnhout, Polym. Degrad. Stab., 2007, 92, 1247–1254
50. A. L. Kioniksen and B. Nystrom, Macromolecules, 1996, 29, 5215–5222
51. J. W. Teh, H. P. Blom and A. Rudin, Polymer, 1994, 35, 1680–1687
52. Y. P. Khanna, Macromolecules, 1993, 26, 3639–3643
53. C. Carrot, J. Guillet and K. Boutahar, Rheol. Acta, 1993, 32, 566–574
54. S. Vleeshouwers, A rheological study of shear induced crystallization, Rheol. Acta, 1996, 35, 391–399
55. W. Nagatake, T. Takahashi, Y. Masubuchi, J. I. Takimoto and K. Koyama, Polymer, 2000, 41, 523–531
56. Y. Masubuchi, K. Watanabe, W. Nagatake, J. I. Takimoto and K. Koyama, Polymer, 2001, 42, 5023–5027
57. S. A. Madbouly and T. Ougizawa, J. Macromol. Sci., Part B: Phys., 2003, 42, 269–281
58. S. Iannace, A. Maffezzoli, G. Leo and L. Nicolais, Polymer, 2001, 42, 3799–3807